The Journal of Neuroscience, June 1994, 14(6): 3922–3933

Comparison of Mammalian Adult and Fetal Nicotinic Acetylcholine Receptors Stably Expressed in Fibroblasts

Carrie Kopta and Joe Henry Steinbach

Department of Anesthesiology, Washington University School of Medicine, St. Louis, Missouri 63130

Cells from a line of transformed quail fibroblasts (QT-6) were transfected with cDNAs coding for subunits of the mouse muscle nicotinic ACh receptor (AChR). Stable clones were selected that expressed subunits of the fetal-type AChR (α, β, γ, δ) or the adult-type AChR (α, β, ϵ, δ). The receptors had the appropriate burst durations and single-channel conductances for the fetal or adult type, respectively. Each type of receptor had a dose–response relationship that was close to a square law at low concentrations of ACh, implying that they contained two ACh-binding subunits. The metabolic stability of surface fetal and adult receptors was identical (about 10 hr half-life), for two independent clones expressing fetal and two expressing adult AChR. The metabolic stability was unaffected by treatment with okadaic acid, which enhanced receptor phosphorylation. *d*-Tubocurarine (dTC) blocked both the binding of α-bungarotoxin (BTX) to the cells and the ACh-elicited current. dTC blocked BTX binding with indistinguishable efficacy for both fetal and adult AChR. However, it was sixfold less effective at blocking ACh-elicited current from fetal AChR. At least part of the difference results from the ability of fetal receptor channels to open when the receptor has one ACh and one dTC molecule bound, whereas channels of heteroliganded adult receptors do not open. The data indicate that the subunit composition directly affects physiological and pharmacological properties of muscle AChR, but has little effect by itself on metabolic stability.

[Key words: ACh receptor, synapse, muscle development, metabolism, curare, phosphorylation]

Nicotinic ACh receptors (AChR) are highly concentrated in the postsynaptic region of the neuromuscular junction. During development the shape and resistance to disruption of the aggregate of AChR proceed through a series of changes (see Steinbach and Bloch, 1986). Over the same period, although at different times, the metabolic stability of the AChR at the junction increases and the pharmacological and physiological properties of the junctional AChR change (Schuetze and Role, 1987). Molecular cloning and expression of subunits for mammalian AChR have shown that a major determinant of the physiological changes during development is the subunit composition of the AChRs (Mishina et al., 1986). Adult junctional AChR contain α, β, δ, and ϵ subunits. The receptors at fetal junctions, and the extrajunctional AChR synthesized by denervated adult muscle fibers contain α, β, δ, and γ subunits. Analysis of the physiological properties of AChR expressed in *Xenopus* oocytes after injection of purified mRNA for specific subunits has shown that a receptor composed of α, β, δ, and γ subunits has the lower conductance and longer burst duration of fetal-type AChR, whereas one composed of α, β, δ, and ϵ subunits has the higher conductance and briefer duration characteristic of the adult junctional type (Mishina et al., 1986). The junctional AChR at the early stages of development have the physiological properties of fetal-type AChR (Schuetze and Role, 1987). However, it is not clear whether other properties of the junctional AChR that change during development also are influenced by the subunit composition. To examine this question, we have generated stably transfected nonmuscle cells that express fetal- and adult-type AChR (Phillips et al., 1991).

The AChR at the adult neuromuscular junction are metabolically much more stable than those at fetal junctions or in the extrajunctional regions of denervated adult fibers (a half-life of about 400 hr compared to one of about 20 hr; Reiness and Weinberg, 1981; Bevan and Steinbach, 1983). During development, the metabolic stability of the junctional receptors increases over a period when the individual AChR retain the kinetic properties of fetal-type AChR (Reiness and Weinberg, 1981), which suggests that subunit composition does not directly affect metabolic stability. However, Gu et al. (1990) found that when adult- or fetal-type AChR were transiently expressed in COS cells, the adult type were degraded at only half the rate of fetal, indicating a direct influence of subunit composition on stability. The metabolic stability of junctional receptors can be decreased; after denervation of an adult muscle, the AChR that had been located at the junction become more rapidly degraded (Loring and Salpeter, 1980; Bevan and Steinbach, 1983). This change can be reversed in organ-cultured muscle by treating the muscle with drugs that should increase the level of protein phosphorylation by protein kinase A (Shyng et al., 1991). Since the AChR are of the adult type, the possibility exists that phosphorylation differentially affects the metabolic stability of fetal and adult receptors.

It has also been reported that the neuromuscular blocking agent *d*-tubocurarine (dTC) is less effective at reducing ACh-elicited responses in denervated fibers (which express fetal-type receptors) than innervated fibers (Jenkinson, 1960; Beranek and Vyskocil, 1967). The basis for this difference is not known but it could reflect the affinity of dTC for the two types of AChR.

Received June 1, 1993; revised Dec. 6, 1993; accepted Jan. 13, 1994.

We thank Drs. P. Blount, J. Merlie and W. Phillips for advice and vectors, C. Ifune, C. Lingle, D. Maconochie, J. Merlie, W. Phillips, and J. Zempel for reading the manuscript, and M. Privalsky. This research supported by National Institutes of Health grant NS 22356 and a grant from the McDonnell Center for Cellular and Molecular Neurobiology.

Correspondence should be addressed to J. H. Steinbach, Department of Microbiology, University of California, Davis
Davis, CA 95616.

There are conflicting reports of the ability of dTC to occupy ACh-binding sites and thereby reduce the binding of the snake neurotoxin α-bungarotoxin (BTX). In one study of dTC binding to AChR extracted from innervated and denervated fibers, dTC apparently bound more tightly to adult AChR (Brockes and Hall, 1975), but other studies found no difference (Colquhoun and Rang, 1976; Kemp et al., 1980). A study of fetal and adult AChR transiently expressed in COS cells found that dTC bound equally well to both types (Gu et al., 1990). The binding data suggest that the earlier physiological studies that showed a difference in block by dTC might be the result of some of the many possible technical problems associated with studies of functional block.

Materials and Methods

Materials. Chemicals were obtained from Sigma Chemical (St. Louis, MO) unless otherwise specified. Phosphate-buffered saline (PBS) contained (in mM) 140 NaCl, 2.7 KCl, 9.6 PO_4, pH 7.4. Earle's Balanced Salt Solution (EBSS) contained 116 NaCl, 5.4 KCl, 1.8 $CaCl_2$, 0.8 $MgSO_4$, 26 $NaHCO_3$, 1 NaH_2PO_4, 5.5 glucose, pH 7.4. Complete growth medium was 199 Earle's medium with 10% (v/v) tryptose phosphate broth (TPB; GIBCO, Grand Island, NY), 5% fetal bovine serum (FBS; Hyclone, Logan, UT), 1% dimethyl sulfoxide ($MeSO_2$), 100 U/ml penicillin, 100 μg/ml streptomycin.

Transfections and cell culture. The transformed quail fibroblast cell line QT-6 was maintained, transfected, and stable clones isolated as described earlier (Phillips et al., 1991). Cells were grown in complete growth medium and maintained at 37°C in a humidified 5% CO_2, 95% air atmosphere. Briefly, QT-6 cells were cotransfected with a mixture of four plasmids containing the mouse muscle cDNAs for subunits of fetal- (α, β, γ, δ) or adult- (α, β, ε, δ) type muscle acetylcholine receptor (AChR) and a plasmid containing the gene for neomycin resistance, neo. Each gene was under the control of the Rous sarcoma virus long terminal repeat promoter in separate expression constructs previously described (Phillips et al., 1991). Approximately 24 hr following transfection using calcium phosphate precipitation/glycerol shock (Graham and Van Der Eb, 1983), the cells were removed from the dish by light trypsinization, resuspended in complete growth medium containing 300 μg/ml geneticin (GIBCO), and replated at one-half the original density. Colonies resistant to geneticin were isolated and screened on the basis of surface ^{125}I-α-bungarotoxin (^{125}I-BTX) binding (Sine and Taylor, 1979). Isolated clones were maintained in complete growth medium containing 150 μg/ml geneticin. Two clones were derived from colonies of cells transfected with α, β, γ, and δ subunits (Q-F18 and Q-F17) and two from colonies of cells transfected with α, β, ε, and δ (Q-A33 and Q-A8). Q-F18 and Q-A33 clones were used for most studies, as they expressed slightly higher levels of AChR.

Metabolic labeling and immunoprecipitation. Five millimolar sodium butyrate was added to confluent 10 cm dishes of Q-A33 and Q-F18 cells 2 d prior to metabolic labeling to enhance AChR expression and was included in the "pulse" and "chase" media. Metabolic labeling and immunoprecipitation of solubilized AChR were generally performed as described previously (Covarrubias et al., 1989). Quail fibroblasts were labeled with 130 μCi of ^{35}S-methionine in 199 Earle's medium without methionine supplemented with 10% (v/v) TPB, 5% dialyzed FBS, 1% $MeSO_2$, and 10 μM unlabeled methionine. BC3H-1 cultures were labeled with 100 μCi of ^{35}S-methionine, in Dulbecco's Modified Eagle's Medium without methionine, supplemented with 5% dialyzed FBS and 10 μM unlabeled methionine. Following the 1 hr pulse, the radioactive medium was replaced with the appropriate complete growth medium supplemented with 1 mM methionine and 10 nM BTX for a 3 hr chase. The cell monolayers were washed three times with wash buffer 1 [WB1: PBS plus 300 μM phenylmethylsulfonyl fluoride (PMSF) and 5 mM EDTA]. Cells were scraped from the dish and pelleted in the third wash, the supernatants were aspirated, and the cell pellets frozen at −80°C. All subsequent steps were conducted at 4°C or on ice. The pellets were thawed into WB1, repelleted, and washed again. Cells were solubilized with a 15 min incubation while rocking at 4°C in extraction buffer (100 μg/ml each leupeptin, antipain, and soybean trypsin inhibitor, 10 μg/ml each of pepstatin and aprotinin, 0.2 U/ml α-2-macroglobulin, 200 μM PMSF, 5 mM each EDTA and EGTA, 1% TX-100 in 150 mM NaCl, 50 mM Tris, pH 8.2). The extracts were centrifuged for 10 min in an Eppendorf microfuge and the supernatants collected. Supernatants were "precleared" by incubation with anti-mouse and anti-rat antibody preabsorbed to fixed *Staphylococcus aureus* (Immunoprecipitin; Bethesda Research Labs, Gaithersberg, MD) with rocking for 30 min. Immunoprecipitin was removed by centrifugation in a microfuge. Surface AChR was immunoprecipitated with anti-BTX antiserum generally as described (Smith et al., 1986; Covarrubias et al., 1989). The cell extract was adjusted to 500 mM NaCl, and Protein-A agarose (Boehringer) was used to precipitate. Pellets were washed three times with PBS plus 300 mM PMSF, 5 mM EDTA, 0.5% TX-100 and with 500 mM NaCl, and then twice with 0.1% TX-100 in PBS. For reimmunoprecipitations, AChR was dissociated and eluted from the pellets by heating to 90°C for 5 min in 1% SDS in PBS. The supernatant was adjusted to a final composition of 0.25% SDS, 1.9% TX-100 in PBS, and then subunit-specific antibodies were used to precipitate individual subunits. The monoclonal antibodies used were mAb 61 (α; Tzartos et al., 1981), mAb 148 (β; Tzartos et al., 1981), and mAb 88B (δ; Froehner et al., 1983). Following the final immunoprecipitation, proteins were eluted at 37°C in 2× SDS buffer (SDS buffer: 2% SDS, 10% glycerol, 62.5 mM Tris, pH 6.8). Gel electrophoresis and fluorography were performed as previously described (Covarrubias et al., 1989), except that signal enhancement was achieved with Fluorohance (Research Products International, Mount Prospect, IL). For digestion with Endoglycosidase-H (Boehringer Mannheim, Indianapolis, IN), proteins were eluted in 0.4% SDS in PBS. Digestion was performed overnight at 37°C, following the supplier's recommendations.

Cells were labeled with ^{32}P in Dulbecco's Modified Eagle's Medium without P_i, supplemented with 0.1 mM P_i, 0.25 mCi/ml ^{32}P, 1% dimethyl sulfoxide, and 5 nM BTX for 20 hr (Smith et al., 1987). At that time okadaic acid (10 nM final concentration) or forskolin (8 μM with 35 μM RO 20-1724) was added and the cells incubated 1 hr longer. Cells were then washed three times with ice-cold PBS and scraped in buffer (WB2: 20 mM $NaPP_i$, 100 mM NaF, 300 μM PMSF, 5 mM EDTA in PBS). Cells were pelleted, the supernatant was aspirated, and then the pellet was frozen at −80°C. For extraction, cells were thawed on ice in WB2 and washed once, then extracted in modified extraction buffer (all inhibitors as above, but with 3 μg/ml RNase A added and Tris and NaCl replaced by 20 mM NaP_i, 20 mM $NaPP_i$, and 100 mM NaF, pH 7.5). Immunoprecipitations were performed as described above, but pellets were washed with 20 mM $NaPP_i$, 100 mM NaF, 500 mM NaCl, 5 mM EDTA, 0.5% TX-100 in PBS. The final wash before elution with SDS buffer was performed with 20 mM $NaPP_i$, 60 mM NaF, 0.1% TX-100 in PBS.

Ligand binding assays. The quantity of surface BTX-binding sites was determined essentially as described (Covarrubias et al., 1989). Monolayers were labeled with 10 nM ^{125}I-BTX for 2 hr at room temperature or 1 hr at 37°C, washed, removed from the dish by scraping or solubilization with 0.1 M NaOH and counted on a counter. Nonspecific binding was estimated by addition of 1 μM unlabeled BTX to the labeling medium and subtracted from total binding to give specific binding. BTX-binding sites were converted to numbers of AChR assuming that two BTX molecules bound per AChR.

Inhibition of the initial rate of BTX-binding by *d*-tubocurarine (dTC) or carbamylcholine (CCh) was determined as described by Sine and Taylor (1979). Confluent 35 mm dishes of Q-A33 or Q-F18 cells were treated with 2 mM sodium butyrate for 2 d. Monolayers were preincubated for 10 min at room temperature with the appropriate concentration of dTC or CCh in EBSS plus 0.2% FBS and 120 mM glucose. This solution was aspirated and replaced with an identical solution containing 10 nM ^{125}I-BTX. After incubation at room temperature for 15 min the cells were washed three times, removed from the dish with 0.1 M NaOH, and counted in a γ-counter.

Degradation of surface AChR. The metabolic half-life of surface AChR was determined as in Patrick et al. (1977). Confluent cultures (not treated with sodium butyrate) were labeled for 1 hr at 37°C with 10 nM ^{125}I-BTX in complete growth medium. After labeling, cells were washed three times with prewarmed growth medium, and then incubated for the indicated times. Nonspecifically bound ^{125}I-BTX was determined by preincubating sister cultures with 1 μM unlabeled BTX, as described earlier. At each time point, the culture medium was collected and the monolayer was washed once with growth medium. The medium and rinse were pooled to estimate the released radioactivity at that time, and cells were removed from the dish with 0.1 M NaOH to estimate the retained radioactivity. Forskolin or okadaic acid (Kamiya Biomedical, Thousand Oaks, CA) was included in the labeling, incubation, and

wash media when used. RO 20-1724 (a gift from Dr. J. Lawrence, Washington University School of Medicine) was included only in the labeling and incubation media due to a limited supply of this reagent.

Autoradiography. Cultures were labeled for autoradiography using the protocols described above to determine total and nonspecific binding. Cultures were fixed with 4% paraformaldehyde (w/v in PBS) for 20 min, and processed as described in Steinbach (1981). Grains were counted at 400× over a square 12 × 12 μm centered over randomly selected cells, and converted to AChR densities assuming two BTX-binding sites per AChR and an emulsion efficiency of 0.5 grains per γ emission (Steinbach, 1981). Background grain densities were counted over regions of the dish that did not have cells or over autoradiographs of cultures that had been pretreated with unlabeled BTX, and were 20% or less of the mean grain density over cells.

Physiological recordings. Recordings were made using cell-attached, whole-cell, or excised patch configurations of the patch-clamp method (Hamill et al., 1981). Recordings were made at room temperature. Data were recorded on digital tape, then played back, filtered, and then digitized and analyzed using a 386-based computer. Burst durations were determined from cell-attached recordings using 300 nM ACh, from cells depolarized with a high K^+ bath solution so that the membrane potential was set by the pipette potential. The reversal potential determined in these conditions was close to 0 mV (Q-A33: −1.0 ± 3.2 mV, 11 cells; Q-F18: −0.1 ± 2.7 mV, 9 cells), indicating that the resting potential was close to 0. Data were filtered at 2000 Hz, detecting transitions using a half-maximal threshold crossing method and defining bursts with a 2 msec maximal closed time within bursts. Whole-cell currents were recorded at −50 mV in Na^+ external saline (see below) with 0.5 mM Ca^{2+} added, unless otherwise specified. Agonist-elicited whole-cell currents were measured as the difference between the means of 3–5-sec-long data segments taken preceding the application and at the peak of the response.

All recording solutions contained 20 mM HEPES and were adjusted to pH 7.3 using the appropriate monovalent cation hydroxide salt. Solutions contained 20–25 mM glucose, to bring the measured osmolarity to 320–330 mOsm. Sodium external solution contained (in mM) 140 NaCl, 2 KCl, and no added divalents; cesium external solution contained 140 CsCl; potassium external solution contained 140 KCl. The internal solution contained 140 CsCl, 1 $MgCl_2$, and 2 EGTA. Drugs were dissolved in the appropriate external solution and applied using a local perfusion system (Konnerth et al., 1987), which allowed changes to be made in about 0.5 sec. All ACh solutions applied to cells or to outside-out patches contained 300–600 nM atropine sulfate. Atropine was omitted from pipettes when burst durations were to be measured. Drugs were maintained as frozen stocks and appropriate dilutions were made up on the day of the experiment.

As will be described in Results, the number of surface receptors differed among individual cells. For many of the physiological experiments cells with a high and relatively consistent surface density were chosen by labeling cells with tetramethyl-rhodamine–conjugated Fab fragments of the monoclonal antibody mAB-35. The mAB-35 hybridoma was obtained from the American Type Culture Collection (Gaithersberg, MD), and purification, digestion, and labeling of the immunoglobulin were performed using standard methods (Harlow and Lane, 1988). mAB-35 binds to an external epitope on the α subunit of muscle AChR and has been reported to have no effect on the functional properties of AChR isolated from *Torpedo* electric organ (Blatt et al., 1985). No effects were noted in comparisons of single-channel conductances or channel burst durations measured on stained or unstained fibroblasts (data not shown). However, use of this method for identifying cells increased the odds of obtaining records that provided adequate levels of activity. In 123 recordings using 400–1000 nM ACh from randomly chosen cells, 34% of the patches showed no AChR activity over a 1–2 min recording period, 31% showed very low activity (<1 burst/min), 28% showed activity ranging from 5 to 100 bursts/min, and the remaining 7% showed high activity with most of the record showing overlapping openings. For patches on 42 cells selected for high mAB-35 binding, 11% showed very low activity, 69% showed activity at about 20–100 bursts/min, and the remaining 19% showed multiple overlapping openings.

Data analysis. Equations were fit to data curves using a nonlinear fitting program (NFITS, kindly provided by Dr. C. Lingle, Washington University School of Medicine). Protection curves were fit with the Hill equation $[Y = 1/(1 + [X/K_D]^n)]$, or by a curve described by the sum of occupancies of two independent sites of different affinity present in equal amount $[Y = 0.5/(1 + [X/K_{D1}]) + 0.5/(1 + [X/K_{D2}])]$. Blocking curves were fit with the Hill equation. Single-channel conductances were determined by fitting straight lines to single-channel current–voltage relationships over the range of −20 mV to −140 mV. Degradation curves and the voltage dependences of mean burst duration were analyzed by fitting single exponential curves to the data. All results are presented as mean ± standard deviation.

Results

Quail fibroblast (QT-6) cells were transfected with cDNAs for subunits of mouse muscle nicotinic AChR. Clonal lines expressing high levels of fetal AChR (Q-F18, transfected with α, β, γ, and δ subunits) and adult AChR (Q-A33, transfected with α, β, ε, δ subunits) were established. Two lines established from separate colonies (Q-F17 and Q-A8) were used for some studies.

In confluent cultures Q-F18 cells expressed 10,000 ± 6000 (mean ± SD, $N = 6$) surface AChR per cell, while Q-A33 expressed 7000 ± 4000 ($N = 7$). Sodium butyrate, in many cells, causes cell cycle arrest and inhibits histone deacetylase, resulting in histone hyperacetylation (Kruh, 1982; Charollais et al., 1990). It has been used to increase transfection efficiencies and to enhance transcription of exogenous DNA (Gorman and Howard, 1983). Treatment with sodium butyrate resulted in an increase in the surface expression of AChR (cf. Sine and Claudio, 1991a). In our hands, 10 mM butyrate proved to be toxic to cells, but treatment of confluent cultures with 2 mM for 2 d or 5 mM for 1 d resulted in 2.6-fold (±0.7; Q-F18, $N = 5$) and 4.7-fold (±1.1; Q-A33, $N = 3$) increases in the numbers of surface AChR per cell. Cell growth at 30°C for 1–2 d slightly reduced receptor expression (cf. Sine and Claudio, 1991a). Butyrate-treated cultures were used for studies of subunit composition and BTX-binding, but not for studies of AChR metabolism.

Subunit composition of surface AChR

The apparent molecular weights of subunits of surface AChR expressed by Q-F18 and Q-A33 cells were compared to those of mouse subunits expressed by clonal BC3H-1 cells (Fig. 1). BC3H-1, Q-F18, and Q-A33 cells were metabolically labeled with ^{35}S-methionine and BTX was bound to surface AChR on intact cells, as described in Materials and Methods. Toxin–AChR complexes were solubilized, and the surface AChR were precipitated with anti-BTX antibody. The identity of the α, β, and δ subunits was confirmed by elution from the initial pellet and reprecipitation with subunit-specific antibodies (data not shown).

The α and β subunits expressed in all three cell lines have the expected apparent molecular weights of approximately 40 kDa and 48 kDa, respectively. Treatment of immunoprecipitated subunits from BC3H-1, Q-F18, and Q-A33 cells with Endoglycosidase-H, which removes high mannose carbohydrate moieties, resulted in faster migration of α and β subunits with apparent molecular weights of about 37 kDa and 46 kDa. These results suggest that the α and β subunits expressed in fibroblasts are glycosylated and contain primarily high mannose chains, as expected from work with BC3H-1 cells (Smith et al., 1986; Covarrubias et al., 1989) and *Torpedo* electroplax (Nomoto et al., 1986).

The γ and δ subunits are difficult to isolate and resolve into discrete bands as they are susceptible to proteolysis (Smith et al., 1986; Forsayeth et al., 1990; Gu et al., 1990). They also have substantial complex oligosaccharide content (Nomoto et al., 1986). The subunits synthesized by the fibroblast cells have a slightly larger apparent molecular weight than those of BC3H-1 cells (about 68 kDa vs 64 kDa; Fig. 1). The apparent molecular

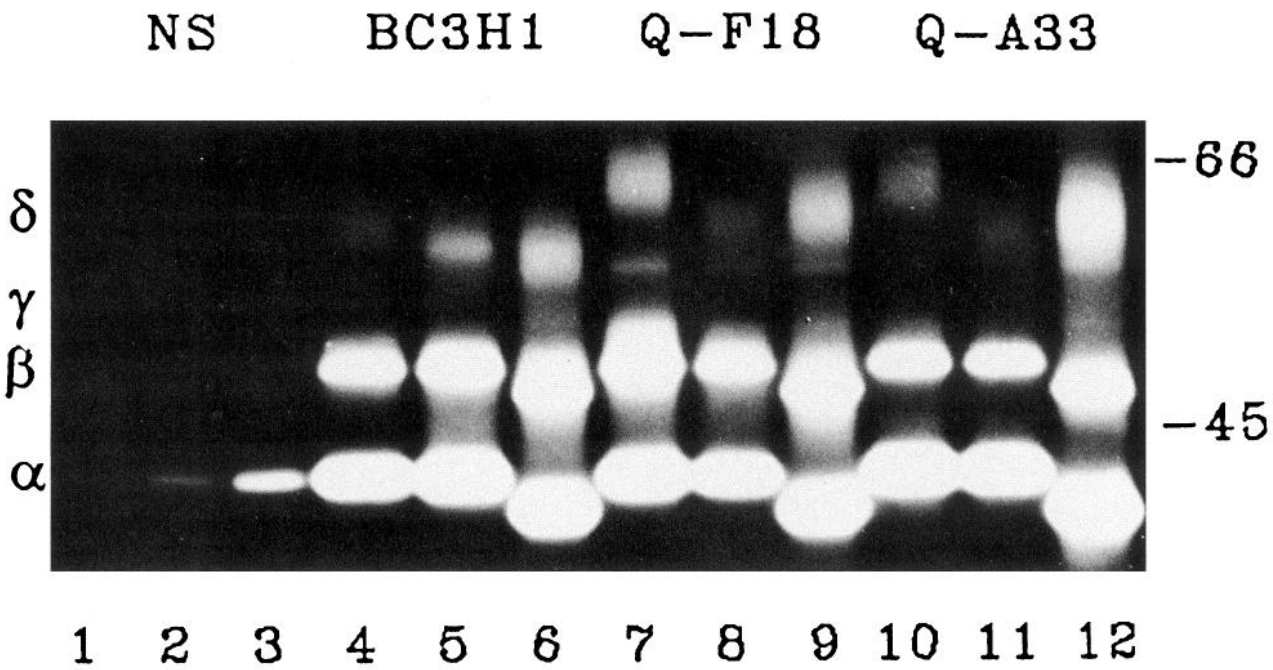

Figure 1. Subunit composition of surface receptors. Proteins of fibroblasts and BC3H-1 cells were labeled by incorporation of ^{35}S-methionine, and then BTX was bound to the surface AChR of intact cells. The toxin–AChR complex was precipitated by anti-BTX, and the precipitated proteins resolved on SDS-PAGE. The figure shows proteins precipitated from BC3H-1 (*lanes 4–6*), Q-F18 (*lanes 7–9*), and Q-A33 (*lanes 10–12*) cells. The proteins were precipitated from control cells (*lanes 4, 7,* and *10*) and from cells grown in the presence of swainsonine (*lanes 5, 8,* and *11*). Extracts from control cells were also treated with Endoglycosidase-H; the precipitated proteins are shown in *lanes 6, 9,* and *12*. Nonspecifically precipitated proteins are shown on the left (*NS*; *lane 1*, BC3H-1; *lane 2*, Q-F18; *lane 3*, Q-A33). The approximate position of the subunits is shown on the left: note that the γ subunit runs very closely above the β subunit in the extracts from BC3H-1 (*lane 4*) and Q-F18 (*lane 7*) cells, and that the position of the ϵ subunit is not known.

weight of the δ subunits is reduced by growth of cells in the presence of swainsonine (an inhibitor of α-mannosidase II; to 60 kDa for BC3H-1 cells and 62 kDa for fibroblasts) and by treatment with Endoglycosidase H (to about 60 kDa for BC3H-1 cells and 64 kDa for fibroblasts). These observations suggest that the metabolism of complex carbohydrates on glycoproteins differs slightly between the quail fibroblasts and BC3H-1 cells.

Since adult- and fetal-type AChR are distinguishable based on physiological properties, we relied on electrophysiological recordings to confirm the presence of the ϵ subunit.

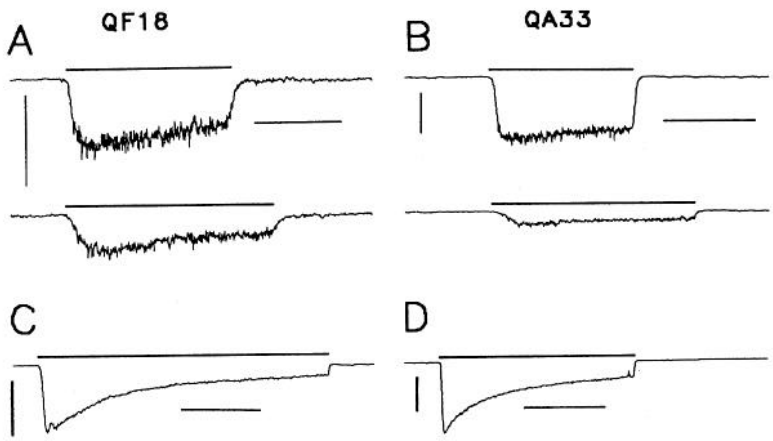

Figure 2. Responses of fibroblasts to cholinergic agents. Whole-cell current responses are shown for Q-F18 (*A* and *C*) and Q-A33 cells (*B* and *D*). In *A* and *B* 400 nM ACh alone was applied to a cell (*upper traces*; time of application shown by the *bar above traces*) or 400 nM ACh plus 200 nM dTC was applied to the same cell (*lower traces*). dTC is clearly more efficacious at reducing the response of the Q-A33 cell (82% block; compare traces in *B*) than the Q-F18 cell (40% block; *A*). In *C* 20 μM CCh was applied to a second Q-F18 cell and in *D* to a second Q-A33 cell. In each case a desensitizing current is elicited. The decay of the currents could be described by the sum of two exponential curves declining to a steady current. The time constants of the two exponentials were 5.3 ± 1.3 sec and 47 ± 25 sec (N = 4, Q-A33), and 4.0 ± 1.9 sec and 57 ± 77 sec (N = 3, Q-F18). The slow component accounted for about half of the total amplitude (56 ± 12% for Q-A33 and 47 ± 10% for Q-F18) and the final maintained current was about 10% of the peak (8 ± 8% and 15 ± 13%). Data in *A* and *B* were filtered at 20 Hz and sampled at 50 Hz, and data in *C* and *D* were filtered at 10 Hz and sampled at 10 Hz. Calibration: *A* and *B*, 50 pA, 5 sec; *C* and *D*, 200 pA, 20 sec.

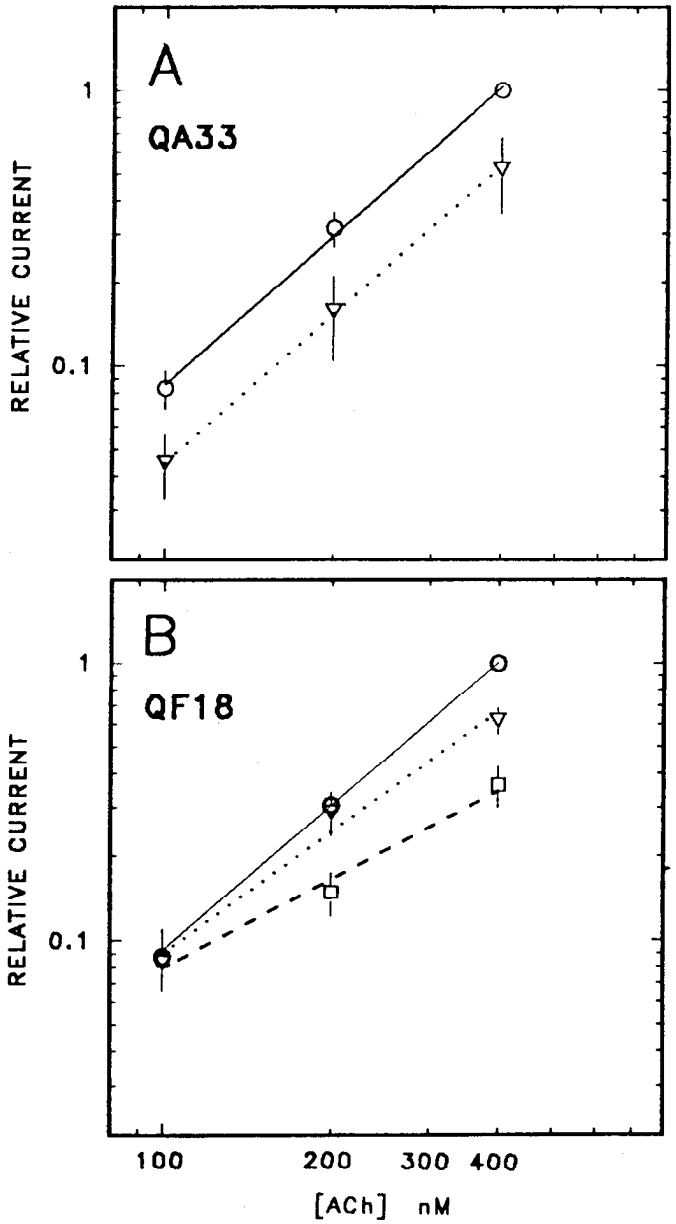

Figure 3. At low [ACh] the dose–response relationship follows a square law. Logarithmic plots of the mean response against the ACh concentration are shown for Q-A33 cells (*A*) and Q-F18 cells (*B*). The responses are normalized to the response to 400 nM ACh given by a cell. The symbols show the mean (±SD) normalized response to ACh (*circles*), and to ACh applied in the presence of 40 nM dTC (*triangles, A* and *B*) or 400 nM dTC (*squares, B*). The *lines* show the mean of the linear regression fits to individual data for cells. For both Q-F18 and Q-A33 cells, the slope in control conditions is close to 2 (*solid line, circles*): for Q-A33 cells the slope is 1.8 ± 0.1 (mean ± SD; 12 cells), and for Q-F18 cells the slope is 1.7 ± 0.1 (11 cells). Forty nanomolar dTC reduces the responses of Q-A33 cells equivalently at all ACh concentrations (by about 50%; *A*), and the slope in the presence of 40 nM dTC is 1.8 ± 0.05 (*dotted line, triangles*; eight cells). This slope does not differ significantly from control (two-tailed *t* test). For responses from Q-F18 cells (*B*), on the other hand, 40 nM and 400 nM dTC (*squares, dashed line*) have less effect on responses to 100 nM ACh than to 400 nM ACh. With 40 nM dTC, the response to 100 nM ACh is 117 ± 26% of control and the response to 400 nM ACh is 62 ± 7%; with 400 nM dTC the relative responses are 86 ± 12% and 36 ± 6% ($P < 0.01$ in each case that the degree of block is the same at a given dTC concentration). The linear regression slopes are 1.45 ± 0.07 (40 nM dTC; three cells) and 1.05 ± 0.05 (400 nM dTC; four cells). The slopes are significantly different from control in both 40 nM dTC ($P < 0.05$) and 400 nM dTC ($P < 0.01$).

Table 1. Physiology and pharmacology of fetal and adult AChR

	Q-F18	Q-A33
Conductance (pS; no Ca^{2+} or Mg^{2+})		
K	73 ± 4	123 ± 2
Cs	68 ± 3	86 ± 2
Na	54 ± 4	84 ± 3
Na + 0.5 mM Ca^{2+}	3 ± 1	56 ± 5
Burst		
Duration (msec; at −100 mV)	5.7 ± 1.8	1.6 ± 0.5
V dependence (mV^{-1})	119 ± 53	121 ± 31
Dose–response (100–400 nM ACh)		
Slope of log-log plot	1.7 ± 0.1	1.8 ± 0.1
dTC inhibition of current		
K_D (nM)	370	44
n	0.8	1.0
dTC inhibition of BTX-binding		
Hill equation K_D (nM)	690 ± 170	590 ± 50
n	0.7 ± 0.1	0.7 ± 0.1
Two-site K_{D1} (nM)	150 ± 50	170 ± 100
K_{D2}	3000 ± 1200	3000 ± 1200
CCh inhibition of BTX binding		
Hill equation K_D (nM)	17,000 ± 8000	17,000 ± 8000
n	1.8 ± 0.3	1.9 ± 0.4

This table lists physiological and pharmacological properties of the ACh receptors expressed by stably transfected fibroblasts. The single-channel conductances and burst durations were determined from cell-attached patches at negative membrane potentials. Single-channel current depended linearly on membrane potentials between −20 mV and −100 mV; the conductance value is the slope of this relationship. Other parameters were derived from fitting curves presented in Figures 3 and 4. Values are mean ± SD for 3–12 measurements except for the inhibition of ACh-elicited currents by dTC, which is the result of a fit to the data in Figure 5*C*. The conductance for Na^+ in the presence of external Ca^{2+} was reported in Phillips et al. (1991).

Physiological properties of expressed AChR

As expected for a nicotinic ACh receptor, inward currents were elicited by ACh (Fig. 2), carbamylcholine (CCh; Fig. 2), and nicotine (data not shown). Currents were blocked by dTC (Fig. 2), but not by atropine (200–600 nM). Currents reversed near 0 mV and could be carried by Na^+, K^+, or Cs^+ ions.

The low-concentration dose–response relationship was examined by determining the whole-cell response to concentrations of 100, 200, and 400 nM ACh. The slope of a log-log plot of the normalized responses is close to two for both Q-F18 and Q-A33 cells (Fig. 3, Table 1) and did not differ between control and butyrate-treated cells (1.8 ± 0.1 vs 1.7 ± 0.1 for Q-A33; 1.7 ± 0.1 vs 1.7 ± 0.1 for Q-F18). These observations suggest that activatable surface AChR on either cell line have two ACh-binding sites, both of which must be occupied for efficient channel opening.

The receptors found at normal adult junctions have briefer bursts than those at fetal junctions or nonjunctional regions of denervated muscle, and the burst durations for both types of receptor increase when the membrane potential is made more negative. The bursts recorded from Q-A33 cells are briefer at all potentials than those from Q-F18 cells (Fig. 4). Bursts from both cell types are prolonged at more negative potentials (Fig. 4*B,C*). The distributions of burst durations require the sum of more than one exponential component for adequate description (see Fig. 4*B*), which will be studied further in future work.

Monovalent cations pass through the channels of both adult

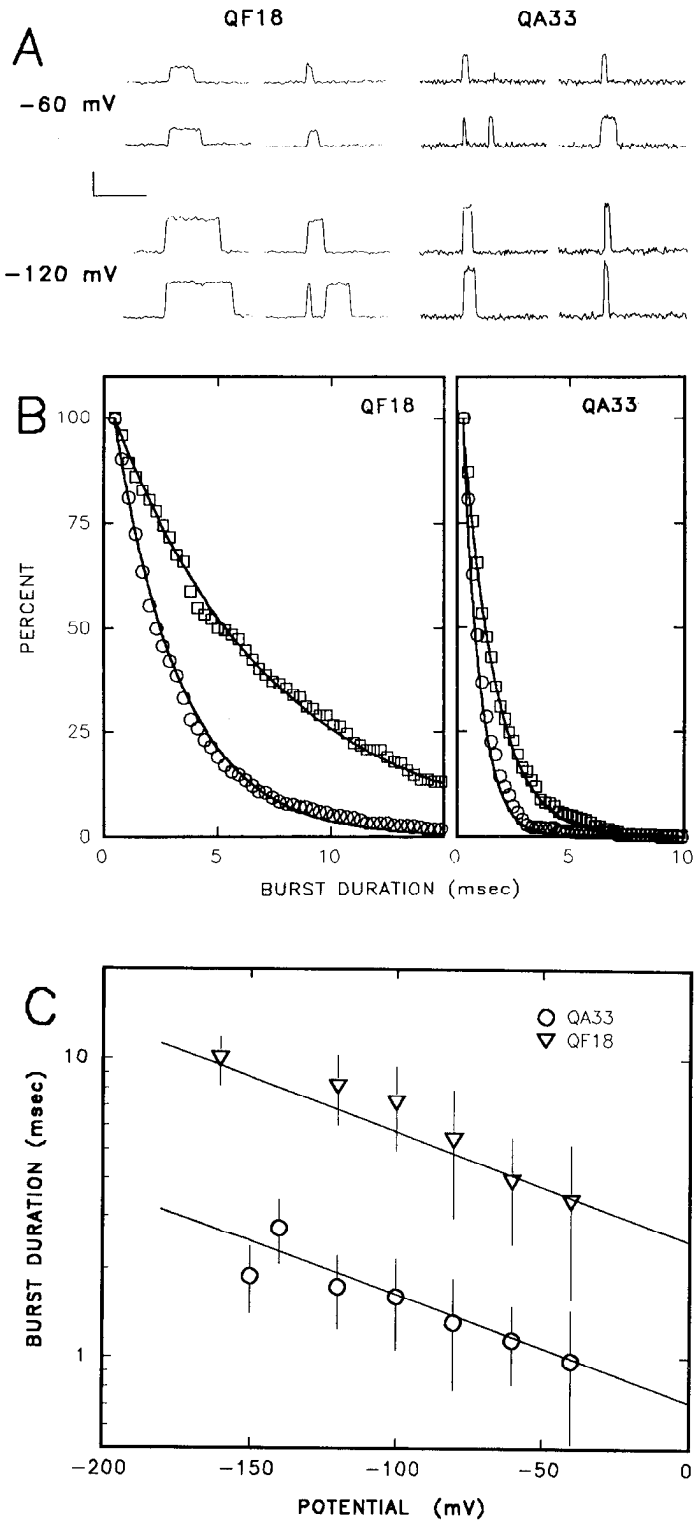

Figure 4. Receptors of Q-F18 cells have a briefer burst duration at all potentials than those on Q-A33 cells. *A*, Single-channel currents elicited by 300 nM ACh were recorded cell-attached from cells depolarized with a high K^+ bath solution. The patch membrane potential during the recording is shown on the *left* (−60 mV upper group, −120 mV lower group). In this recording configuration, currents passing into the cell through an open channel produce upward deflections. Events recorded from Q-F18 cells (*left column*) were of lower amplitude and longer duration than those from Q-A33 cells (*right column*). Calibration: 5 pA, 10 msec. *B*, Burst durations were longer at more negative potentials for both cell types. The figure shows the percentage of bursts (*ordinate*) lasting less than or equal to the time on the *abscissa* (*squares*, −120 mV; *circles* −60 mV). The *lines* show the best-fitting single exponential curve. The total number of entries, arithmetic mean burst duration, and time constant for the best-fitting single exponential are, for Q-F18 at −60 mV, 393 bursts, mean duration 3.7 msec, and time constant 2.9 msec; Q-F18 at −120 mV, 184, 7.6 msec, 7.0 msec; Q-A33 at −60 mV, 373, 1.05 msec, 0.75 msec; Q-A33 at −120 mV, 144, 1.6 msec, 1.4 msec. *C*, The mean burst duration increases at more negative potentials for Q-A33 (*circles*) and Q-F18 cells (*triangles*). The means (±SD) of the mean burst duration for data recorded from two to seven cells at a given potential are shown. The lines show the mean parameters of the linear regression lines fit to data from six Q-A33 and seven Q-F18 cells, with voltage dependences of 121 ± 31 mV and 119 ± 53 mV, respectively, and mean calculated burst durations at −100 mV of 1.6 ± 0.5 msec and 5.7 ± 1.8 msec.

and fetal AChR, while the single-channel conductance of adult receptors is larger. The single-channel conductances for inward currents carried by Na^+, Cs^+, or K^+ ions were measured in solutions containing no added Mg^{2+} or Ca^{2+} ions. The receptors on Q-A33 cells had a larger conductance for each of these ions (Table 1). For both cell types the relative conductances were $Na^+ < Cs^+ < K^+$, although the conductance for the receptors on Q-A33 cells relative to that for receptors on Q-F18 cells was lower for Cs^+ (1.3×) than for Na^+ (1.6×) or K^+ (1.7×).

Pharmacological properties of expressed AChR

Pharmacological properties of the expressed AChR were examined both by a biochemical assay and by studies of drug effects on ACh-elicited currents. The ability of dTC and CCh to reduce the initial rate of BTX-binding provides an estimate for the occupancy of the ACh-binding sites by the drug. There was no difference in the ability of CCh (Fig. 5*A*) or dTC (Fig. 5*B*) to reduce BTX binding to adult- or fetal-type AChR. The concentration dependence of the reduction produced by CCh can be described by the Hill equation with a coefficient greater than 1 (Fig. 5*A*), as has been found in other studies (Sine and Taylor, 1979). The K_D and n_H values were 17 μM and 1.9 for each cell type. This binding curve is thought to reflect CCh-induced desensitization of AChR as well as binding to resting forms of the AChR. When 20 μM CCh is applied to cells, an inward current is elicited that then declines as receptors desensitize (Fig. 2). The desensitization seen was similar in Q-A33 and Q-F18 cells. In both cases the response decayed as the sum of two exponentials to a final steady level at about 10% of the peak response (Fig. 2). At 100 μM CCh or 100 μM nicotine, the responses declined more rapidly and more completely (data not shown).

In contrast to results with CCh, the reduction of the initial rate of BTX-binding produced by dTC shows a Hill coefficient less than 1 (Fig. 5*B*). The concentration dependence of the reduction produced by dTC can also be described by the sum of binding to two sites of differing affinity for dTC that are present in equal numbers (Sine and Taylor, 1981). For both fetal and adult forms of the AChR the high-affinity site had an apparent K_D of about 150 nM and the low-affinity site had a K_D of about 3000 nM (Table 1).

When a low concentration of ACh (400 nM) was applied to cells in the presence of dTC the inward current was reduced for both Q-A33 and Q-F18 cells (Figs. 2, 5*C*). However, the half-blocking concentration of dTC for currents elicited from Q-A33 cells (40 nM) was lower than that for currents from Q-F18 cells (about 300 nM). Three possible explanations for the divergence

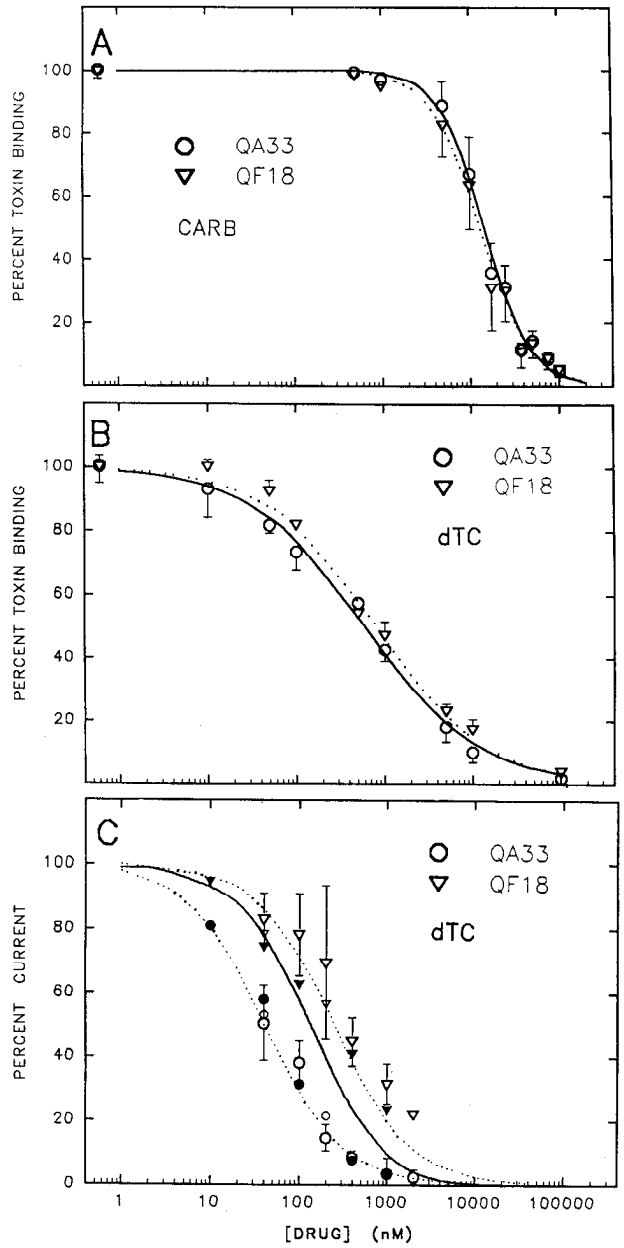

Figure 5. Pharmacological studies on AChR expressed in fibroblasts. *A* and *B* show the ability of various concentrations of CCh (*A*) and dTC (*B*) to reduce the initial rate of binding of BTX to Q-F18 (*triangles*) and Q-A33 (*circles*) cells. Each point shows the mean (±SD) of three determinations of the initial rate normalized to the binding in the absence of added drug. The lines show fits of the Hill equation to the data (*dotted lines*, Q-F18; *solid lines*, Q-A33). For the data obtained with CCh (*A*) the mean (±SD) values were K_D 17 ± 8 μM, n_H 1.8 ± 0.3 (Q-F18) and K_D 17 ± 9 μM, n_H 1.9 ± 0.4 (Q-A33). The mean parameters fit to the data for dTC (*B*) were K_D 690 ± 170 nM, n_H 0.7 ± 0.1 (Q-F18) and K_D 590 50 nM, n_H 0.7 ± 0.1 (Q-A33). The block by dTC could also be described by assuming that two sites of differing affinity were present in equal amount. In this case, the two apparent K_D values were 150 ± 50 nM and 3000 ± 1200 nM (Q-F18), or 170 ± 100 nM and 3000 ± 1200 nM (Q-A33). *C* shows the percentage of control whole-cell current elicited by 400 nM ACh in the presence of various concentrations of dTC plotted against the concentration of dTC used to block the response. Data are shown for control cells (*open symbols*; mean ± SD for data from three to six cells), for cells treated with butyrate (*solid symbols*; mean only shown) and for control cells in EBSS rather than normal recording solution (*small open symbols*; mean only shown). The fit of the Hill equation is shown as *dotted lines* through the data points; the parameters providing the best fit were K_D 370 nM, n_H 0.8 (Q-F18) and K_D 44 nM, n_H 0.95 (Q-A33). For comparison to the binding data (*B*), the *solid line* in *C* shows a plot of the percentage of AChR with no sites occupied by dTC, assuming K_D values of 160 nM and 3000 nM for the two dTC-binding sites.

between the binding and functional data were explored. The shift is not due to an effect of butyrate treatment, as the functional block produced by dTC was identical for each type of cell in control and butyrate-treated cultures (Fig. 5*C*). The shift is also not due to different ionic compositions of the bathing media between binding assays and physiological recordings (cf. Jenkinson, 1960; Fig. 5*C*).

A third possible explanation for the divergence in functional block produced by dTC is that the fetal-type receptors expressed by Q-F18 cells can be activated when a single ACh and a single dTC molecule is bound to a single receptor (i.e., that heteroliganded receptors can be active). This possibility is suggested by previous observations that curariform antagonists can serve as weak activators of fetal-type receptors (Ziskind and Dennis, 1978), and dTC applied alone can elicit small currents from Q-F18 but not Q-A33 cells. When 1000 or 2000 nM dTC was applied to Q-F18 cells the response averaged 4% (±4%, $N = 5$ cells) of the response to 400 nM ACh. In contrast, no response was elicited from Q-A33 cells (five cells tested with no response detected; limit of detection about 0.1%). A prediction of this hypothesis is that applying a dose of dTC that would occupy the high-affinity binding site will reduce the slope of the dose–response relationship for ACh applied to Q-F18 cells. Indeed, if the high-affinity site is saturated by dTC the slope should go to 1. To test this hypothesis, ACh was applied at 100, 200, and 400 nM in the absence of dTC and in the presence of a half-blocking concentration of dTC (40 nM for Q-A33 cells and 400 nM for Q-F18 cells). With adult receptors, the response was reduced with no change in the dose–response relationship for ACh (Fig. 3*A*). In contrast, the slope was significantly reduced for responses from Q-F18 cells (Fig. 3*B*).

Metabolic turnover of surface fetal and adult AChR

The degradation of ^{125}I-BTX bound to surface AChR in Q-A33 and Q-F18 cells was followed as described in Materials and Methods (Fig. 6). There was no significant difference between the half-lives of adult (9.8 ± 2.0 hr) and fetal-type AChR (8.5 ± 0.2). These results were confirmed in studies of two other clones, Q-A8 (11 hr) and Q-F17 (11 hr). In two determinations, 91% and 92% of the radioactivity released from cultures of Q-A33 cells during the first 9 hr was included on P2 gel exclusion chromatography (data not shown), implying that the release reflected degradation of bound ^{125}I-BTX (Devreotes and Fambrough, 1976). Nondegradative loss of BTX from rat muscle AChR is very slow, with a half-life estimated to be 36 d (Bevan and Steinbach, 1983).

Previous studies have shown that the subunits of mammalian (Miles et al., 1986; Smith et al., 1987, 1989) and *Torpedo* AChR (Vandlen et al., 1979) can be phosphorylated. A differential effect of phosphorylation on metabolism of adult- and fetal-type AChR is suggested by the observations of Shyng et al. (1991). Hence, it was of interest to determine whether treatment of Q-A33 and Q-F18 with agents that have been shown to increase phosphorylation levels would result in differential effects on degradation rates. Q-A33 and Q-F18 cultures were treated with 8 μM forskolin plus 35 μM RO20-1724 (an inhibitor of phos-

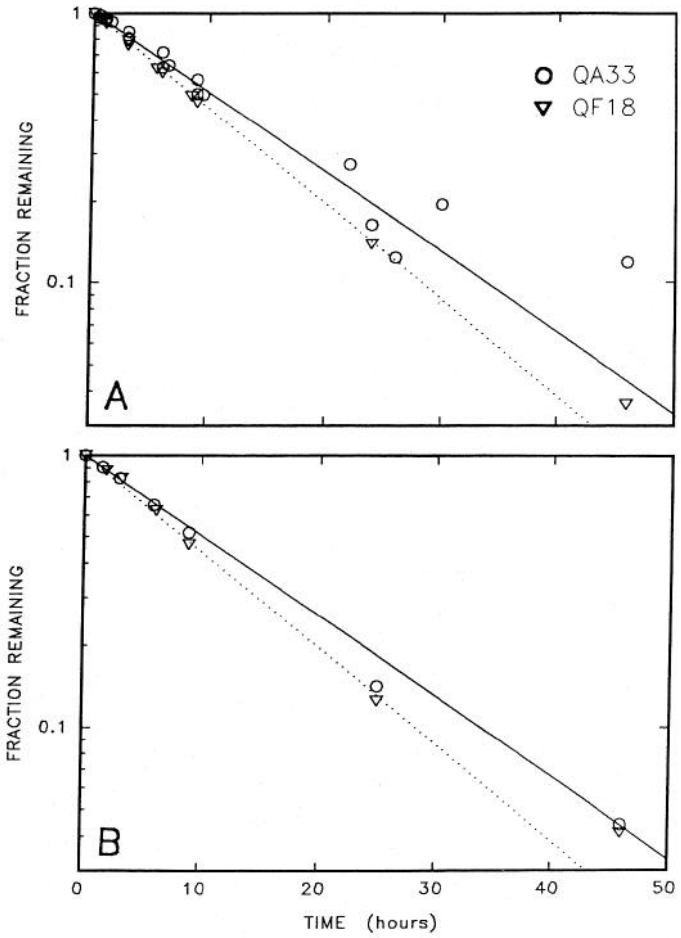

Figure 6. Surface AChR are degraded at similar rates on Q-F18 and Q-A33 cells. Each panel shows the fraction of initially bound ^{125}I-BTX remaining associated with cells, plotted semilogarithmically against time in culture after binding. *A* shows data for control cells; the mean half-life for AChR on Q-F18 cells is 8.5 ± 0.3 hr (N = 2; *dotted line*), and for Q-A33 cells 9.8 ± 2.0 hr (N = 3; *solid line*). *B* shows the lack of effect of okadaic acid treatment (12 nM) on the degradation of AChR of Q-A33 (9.3 hr) and Q-F18 cells (8.5 hr). The lines show mean data for control cells (see *A*).

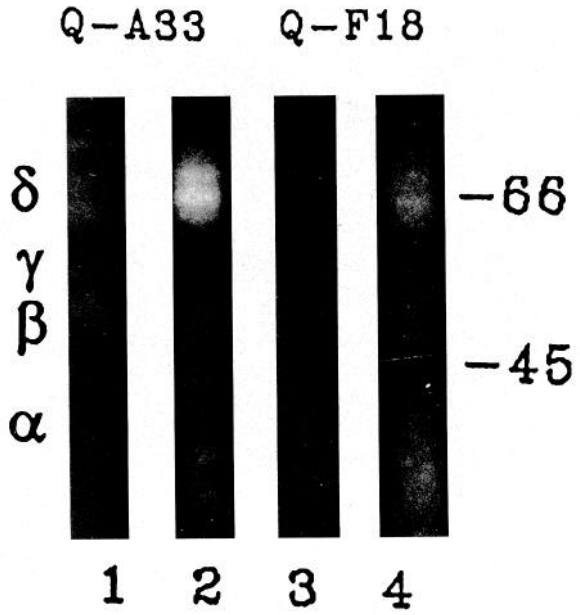

Figure 7. Okadaic acid treatment increases the amount of phosphorylation of the δ subunit in Q-A33 and Q-F18 cells. Cells were labeled with ^{32}P-phosphate and the surface AChR precipitated as described in Materials and Methods. Little radioactivity was incorporated in control cells (*lanes 1* and *3*). After okadaic acid treatment a broad band at about 66 kDa (corresponding to the δ subunit) showed labeling (*lanes 2* and *4*). The locations of α, β, δ, and γ subunits is shown on the left; the ε subunit is not indicated as its apparent molecular weight is unknown.

phodiesterase) or 12 nM okadaic acid (an inhibitor of protein phosphatases-1 and -2A; Cohen et al., 1990) during labeling of cells with ^{125}I-BTX and throughout the time course of degradation. The treatment with okadaic acid increased incorporation of ^{32}P into δ subunit immunoprecipitated from either Q-F18 or Q-A33 cells, as expected (Fig. 7). We were unable to demonstrate increased phosphorylation after forskolin treatment (data not shown). Treatment with okadaic acid had no effect on AChR degradation (Fig. 6*B*), nor did treatment with forskolin (half-life 8.0 hr for Q-A33 and 8.7 hr for Q-F18).

Heterogeneity of receptor expression

It was noted in initial physiological experiments that the whole-cell response to ACh varied from cell to cell. When autoradiographs of cultures that had been incubated with ^{125}I-BTX were prepared, it was clear that some cells showed a higher grain density than others. Averaged over a large number of cells, the calculated mean receptor densities were about 3 AChR/μm² for Q-A33 and Q-F18 cells, and 9 AChR/μm² for BC3H-1 cells (see Fig. 8 caption). These mean values compare reasonably well with those estimated from the specific BTX-binding per cell and measured cell input capacitances (assuming a specific membrane capacitance of 10^{-6} F/cm²), which gave values of 5 AChR/μm² for Q-A33, 6 AChR/μm² for Q-F18, and 30 AChR/μm² for BC3H-1 cells. The agreement between the two estimates of mean receptor density indicates that the autoradiographic densities are not distorted by a systematic artifact (e.g., positive or negative chemography). The distribution of calculated AChR densities on individual BC3H-1 cells is close to Gaussian (Fig. 8*A*) and the mean and median values are quite similar (Fig. 8 caption). The distribution over fibroblasts, in contrast, shows a number of cells with very high density and the mean is several-fold the median (Fig. 8).

The source of this variability does not appear to be due to a polyclonal origin of the cell lines, as similar variability was seen in eight lines subcloned from Q-A33 cells. Similar variability is seen in both confluent and subconfluent cultures, although the proportion of cells with a high density of AChR appears to decrease in postconfluent cultures.

Discussion

We have produced clonal lines of quail fibroblasts that stably express mouse muscle nicotinic ACh receptors of fetal and adult subunit compositions, and have used these lines to compare several properties of these receptors. The surface AChR show components migrating at the expected positions for the α, β, and δ subunits. AChR isolated from Q-F18 cells show, in addition, a band at the position expected for the γ subunit. The apparent molecular weight of the ε subunit is not known, and receptors isolated from Q-A33 cells show only components corresponding to α, β, and δ subunits. The low-concentration dose–response curves indicate that both types of receptor have two

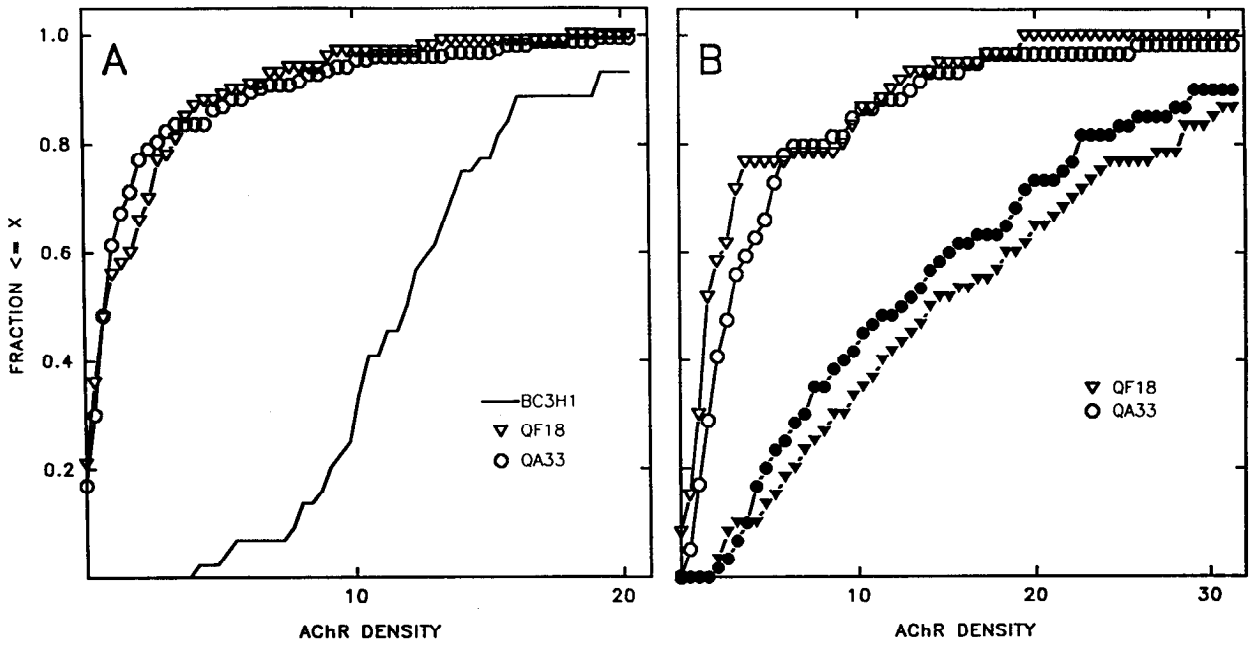

Figure 8. The density of surface AChR differs between cells. The surface AChR density on individual cells was calculated from autoradiographs as described in Materials and Methods. Cumulative plots of the densities for each population (Q-F18, Q-A33, and BC3H-1 cells) are shown here. The *ordinal value* gives the fraction of the total population of cells that has a receptor density less than or equal to the value given on the *abscissa*. BC3H-1 cells show a relatively Gaussian distribution of densities (*A*). Q-F18 and Q-A33 cells, on the other hand, show a higher proportion of cells expressing at low density with a "tail" of cells expressing at much higher density (>5× mean). *B* shows similar plots for control Q-F18 and Q-A33 cells (*open symbols*), and plots for sister cultures treated with 5 mM sodium butyrate for 2 d before binding of ^{125}I-BTX (*solid symbols*). Butyrate treatment results in a shift of the entire distribution to higher levels of expression. The data for *A* are, for Q-F18, $N = 100$, mean density 2.2 ± 3.2 AChR/μm^2, median 0.75; Q-A33, $N = 153$, 2.3 ± 3.8, 0.79; BC3H-1, $N = 44$, 12.3 ± 4.0, 11.9. In *B* grains were counted over 60 cells in each condition, and for Q-F18 control the values were 4.2 ± 5.1, 1.6 and for Q-F18 + butyrate 16.5 ± 9.9, 14; for Q-A33 control 5.3 ± 6.0, 2.9 and for Q-A33 + butyrate 14.5 ± 9.5, 12.4.

ACh-binding sites that must both be occupied for efficient channel opening. Furthermore, Q-F18 cells produce receptors that have a longer burst duration and lower single-channel conductance compared to those produced by Q-A33 cells, as expected from previous studies of fetal and adult muscle AChR. Hence, the surface AChR expressed by Q-F18 cells are likely to have composition $\alpha_2\beta\gamma\delta$ and those by Q-A33 composition $\alpha_2\beta\epsilon\delta$.

Metabolism of surface receptors

The surface receptors on Q-F17, Q-F18, Q-A8, and Q-A33 cells had indistinguishable half-lives, about 10 hr, consistent with the idea that the metabolic stability of muscle AChR is not directly determined by the subunit composition. Our findings differ from the results obtained by Gu et al. (1990), who transiently expressed fetal and adult AChR in COS cells. In this transient expression system, adult AChR had a half-life of 20 hr, about twice as long as fetal AChR. The reason for the difference between our data and that of Gu et al. (1990) is not known, but might reflect differences in the expression systems used.

We found that treatment of cultures with okadaic acid had no effect on metabolic stability of either fetal- or adult-type AChR, although incorporation of phosphate into the AChR δ subunit was enhanced. Forskolin, in our hands, did not enhance subunit phosphorylation in these cells, and also had no effect on metabolism. Shyng et al. (1991) reported that treatment of cultured mouse muscle with forskolin or dibutyryl cAMP had no effect on the metabolic stability of fetal AChR but slowed the degradation of adult AChR; no data on receptor phosphorylation were presented. Our data suggest that increased phosphorylation of the δ subunit has no effect on the metabolic stability of fetal or adult receptors. The δ subunit was the most heavily phosphorylated subunit for both types of receptors, as already reported for the mouse fetal-type receptor expressed by clonal BC3H-1 cells (Smith et al., 1987, 1989). The δ subunit also has the most highly conserved cAMP-dependent phosphorylation site (Huganir and Miles, 1989), suggesting a physiological role for phosphorylation. The ϵ subunit contains a cAMP-dependent phosphorylation site which is absent in mammalian and chicken γ subunit. We were unable to identify the ϵ subunit or to demonstrate a change in its phosphorylation, so we cannot rule out the possibility that the phosphorylation state of the ϵ subunit confers differential stability to adult receptors.

Physiology and pharmacology of surface AChR

The physiological properties are those expected of fetal and adult subunit compositions (cf. Mishina et al., 1986; Schuetze and Role, 1987; Steinbach, 1989). The fetal receptors expressed by Q-F18 cells have a briefer burst duration and lower conductance. The adult and fetal receptors have similar voltage dependences for the burst duration, and both receptor types have relative conductances of $Na^+ < Cs^+ < K^+$.

The fractional occupancy of ACh-binding sites by dTC was assayed by the reduction in the initial rate of BTX binding. In agreement with previous results, the dependence of occupancy on dTC concentration has a Hill coefficient of less than 1; this result has been shown to reflect the fact that the two binding sites have differing intrinsic affinities for curariform antagonists

(Sine and Taylor, 1981). We obtain apparent K_D values of about 150 nM and about 3000 nM, in reasonable agreement with results of others (Sine and Taylor, 1979; Gu et al., 1990). The ability of dTC to reduce the initial rate of BTX binding did not differ for fetal and adult receptors; this agrees with recent observations by Gu et al. (1990).

The most common functional assay for antagonist occupancy of the ACh-binding site is to measure reduction of agonist-elicited ion fluxes or currents. Functional block by dTC and related drugs can be described by a single-site blocking curve with an IC_{50} close to the K_D for the high-affinity site for reduction of the initial rate of BTX binding (Sine and Taylor, 1981), as block of function occurs when either site is occupied by antagonist. Indeed, block of the current elicited by 400 nM ACh occurred at dTC concentrations closer to the K_D for the high affinity site than that for the low-affinity site for both Q-A33 and Q-F18 cells. However, the currents from Q-A33 cells were blocked with an IC_{50} of about 45 nM whereas those from Q-F18 cells had an IC_{50} of about 370 nM. Our data on functional block agree with previous comparisons that found that block of adult-type receptors occurs with an IC_{50} two- to eightfold lower than for fetal AChR (Jenkinson, 1960; Beranek and Vyskocil, 1967). The difference between results obtained on the same type of receptor using different assays likely reflects the fact that dTC is known to be a weak activator of fetal AChR but not adult AChR (Ziskind and Dennis, 1978). This interpretation is supported by our finding that in the presence of a half-blocking concentration of dTC the dose–response relationship for fetal-type receptors for ACh has a slope close to 1. This observation implies that in the presence of this concentration of dTC activation of the receptor follows binding of a single ACh molecule, as would be expected if activation occurred with one dTC and one ACh molecule bound. Adult-type receptors, on the other hand, show no reduction in slope and also show no activation by dTC alone. The hypothesis of heteroliganded activation predicts that the ability of dTC to block ACh-elicited currents in Q-F18 cells will depend on both the ACh and the dTC concentration. This interaction can be seen in the dose–response plots shown in Figure 3. The hypothesis of heteroliganded activation of fetal receptors results in further predictions, some of which have been tested in additional experiments that will be reported elsewhere (J. H. Steinbach, unpublished observations). These results resolve the apparent contradiction between biochemical and functional studies of dTC binding to fetal and adult AchR. The resolution arises because dTC binds indistinguishably, but has different functional actions on fetal and adult AChR.

Comparison to receptors that lack a subunit

These data indicate that the surface receptors have the physiological and pharmacological properties appropriate for fetal or adult AChR. The mean burst durations and mean single-channel conductances differ from those of ACh-elicited currents expressed in *Xenopus* oocytes after injection of mRNA for bovine α, β, and δ subunits (Jackson et al., 1990) or mouse α, β, and γ subunits (Kullberg et al., 1990). Hence, it is unlikely that a large proportion of the functional receptors expressed by the cells have these subunit compositions. Studies also have been made of the ability of dTC to reduce the initial rate of BTX-binding to sites formed by expression of less than the full complement of mouse muscle AChR subunits (Blount and Merlie, 1989, 1991; Sine and Claudio, 1991b). In each case the data are described by the Hill equation with a coefficient close to 1. The site formed by complexes of $\alpha\gamma$, $\alpha\epsilon$, or $\alpha\beta\gamma$ subunits has a K_D close to the high affinity site found on complete AChR, whereas the site formed by $\alpha\delta$ or $\alpha\beta\delta$ subunits has a K_D close to the low-affinity site. Hence, there is no indication that differences between AChR expressed by Q-F18 cells and Q-A33 cells arise from the lack of a subunit in either cell. Rather, the differences most likely arise from the presence of the γ subunit in receptor expressed by Q-F18 cells and the ϵ subunit in AChR expressed by Q-A33 cells.

Cell-to-cell variability in expression

The density of surface AChR expressed by individual cells varied, although the mean number per cell in a population remained constant for many passages. Similar degrees of variability were seen for cultures of Q-A8, Q-A33, Q-F17, and Q-F18 cells. The variability between cells apparently does not result from a polyclonal origin, since similar variability was seen for eight subclones isolated from Q-A33 cells. Also, butyrate treatment appeared to increase the surface AChR density of the entire population of cells. The reasons for this nonuniform phenotype are not known, but a number of studies have made similar observations. For example, fetal-type AChR stably expressed in CHO cells using a β-actin promoter apparently show an identical pattern (Forsayeth et al., 1990). Similar results have been found for inositol-triphosphate receptors (expressed in L cells using a β-actin promoter; Miyawaki et al., 1990), and Epstein-Barr virus antigens (expressed in human lymphoid cell lines using a SV40 promoter; Welinder et al., 1987). Cytoplasmic enzymes also can show similar phenotypic heterogeneity in expression—examples include β-galactosidase (expressed in L cells using the mouse mammary tumor virus promoter; Ko et al., 1990), and human H blood group antigen after transfection of fragments of genomic DNA (presumably encoding fucosyl transferase; L cells, Ernst et al., 1989). Hence, variability in the level of expression between individual cells of a clonal line has been seen for several proteins, in a number of cell types and with a variety of promoters. It is not clear what the basis is for the variability in any of the systems studied.

Summary

One goal of these experiments is to isolate the surface AChR from other muscle-specific proteins, to determine which properties of the AChR expressed at the adult neuromuscular junction (NMJ) result from subunit composition and which are likely to involve additional proteins. Previous work has shown that both fetal and adult receptors are uniformly distributed over the surface of Q-F18 and Q-A33 cells, but both can be aggregated by transient expression of the 43 kDa synapse-associated protein cloned from mammalian muscle cells (Phillips et al., 1991). Our data give no support to the idea that the metabolic stability of surface AChR is affected by the difference in subunit composition between fetal and adult AChR, in distinction to results of a study of receptors transiently expressed in COS cells (Gu et al., 1990). Taking advantage of the accessibility of the expressed AChR for biochemical and biophysical studies, we have confirmed that the binding of dTC is indistinguishable to fetal and adult AChR but that the ability of dTC to block ACh-elicited currents differs. The difference in functional block results, at least in part, from the ability of dTC to serve as a weak activator of fetal receptors. These stable cell lines will prove useful for further studies of muscle nicotinic receptor physiology and regulation.

References

Beranek R, Vyskocil F (1967) The action of tubocurarine and atropine on normal and denervated rat diaphragm. J Physiol (Lond) 188:53–66.

Bevan S, Steinbach JH (1983) Denervation increases the degradation rate of acetylcholine receptors at endplates *in vivo* and *in vitro*. J Physiol (Lond) 336:159–177.

Blatt Y, Montal MS, Lindstrom JM, Montal M (1986) Monoclonal antibodies specific to the β and γ subunits of the *Torpedo* acetylcholine receptor inhibit single-channel activity. J Neurosci 6:481–486.

Blount P, Merlie JP (1989) Molecular basis of the two nonequivalent ligand binding sites of the muscle nicotinic acetylcholine receptor. Neuron 3:349–357.

Blount P, Merlie JP (1991) Characterization of an adult muscle acetylcholine receptor subunit by expression in fibroblasts. J Biol Chem 266:14692–14696.

Brockes JP, Hall ZW (1975) Acetylcholine receptors in normal and denervated rat diaphragm muscle. II. Comparison of junctional and extrajunctional receptors. Biochemistry 14:2100–2106.

Charollais RH, Buquet C, Mesler J (1990) Butyrate blocks the accumulation of CDC2 mRNA in late G1 phase but inhibits both the early and late G1 progression in chemically transformed mouse fibroblasts BP-A31. J Cell Physiol 145:46–52.

Cohen P, Holmes CFB, Tsukitani Y (1990) Okadaic acid: a new probe for the study of cellular regulation. Trends Biochem Sci 15:98–102.

Colquhoun D, Rang HP (1976) Effects of inhibitors on the binding of iodinated α-bungarotoxin to acetylcholine-receptors in rat muscle. Mol Pharmacol 12:519–535.

Colquhoun D, Dreyer F, Sheridan RE (1979) The actions of tubocurarine at the frog neuromuscular junction. J Physiol (Lond) 293: 247–284.

Covarrubias M, Kopta C, Steinbach JH (1989) Inhibition of asparagine-linked oligosaccharide processing alter the kinetics of the nicotinic acetylcholine receptor. J Gen Physiol 93:765–783.

Devreotes PN, Fambrough DM (1976)Turnover of acetylcholine receptors in skeletal muscle. Cold Spring Harbor Symp Quant Biol 15: 237–251.

Ernst LK, Rajan VP, Larsen RD, Ruff MM, Lowe JB (1989) Stable expression of blood group H determinants and GDP-L-fucose: β-D-galactoside 2-α-L-fucosyltransferase in mouse cells after transfection with human DNA. J Biol Chem 264:3436–3447.

Forsayeth JR, Franco A Jr, Rossi A, Lansman JB, Hall ZW (1990) Expression of functional mouse muscle acetylcholine receptors in Chinese hamster ovary cells. J Neurosci 10:2771–2779.

Froehner SC, Douville K, Klink S, Culp WJ (1983) Monoclonal antibodies to cytoplasmic domains of the acetylcholine receptor. J Biol Chem 258:7112–7120.

Gorman CM, Howard BH (1983) Expression of recombinant plasmids in mammalian cells is enhanced by sodium butyrate. Nucleic Acids Res 11:7631–7648.

Graham FL, Van Der Eb AJ (1973) A new technique for the assay of infectivity of human adenovirus 5 DNA. Virology 52:456–467.

Gu Y, Franco A, Gardner PD, Lansman JB, Hall JR (1990) Properties of embryonic and adult muscle acetylcholine receptors transiently expressed in COS cells. Neuron 5:147–157.

Hamill OP, Marty A, Neher E, Sakmann B, Sigworth FJ (1981) Improved patch-clamp techniques for high-resolution current recording from cells and cell-free membrane patches. Pfluegers Arch 391:85–100.

Harlow E, Lane D (1988) Antibodies: a laboratory manual. Cold Spring Harbor, NY: Cold Spring Harbor Laboratory.

Huganir RL, Miles K (1989) Protein phosphorylation of nicotinic acetylcholine receptors. Crit Rev Biochem Mol Biol 24:183–215.

Jackson MB, Imoto K, Mishina M, Konno T, Numa S, Sakmann B (1990) Spontaneous and agonist-induced openings of an acetylcholine receptor channel composed of bovine muscle α-, β-, and δ-subunits. Pfluegers Arch 417:129–135.

Jenkinson DH (1960) The antagonism between tubocurarine and substances which depolarize the motor end-plate. J Physiol (Lond) 152: 309–324.

Kemp G, Morley B, Dwyer D, Bradley RJ (1980) Purification and characterization of nicotinic acetylcholine receptors from muscle. Membr Biochem 3:229–257.

Ko MSH, Nakauchi H, Takahashi N (1990) The dose dependence of glucocorticoid-inducible gene expression results from changes in the number of transcriptionally active templates. EMBO J 9:2835–2842.

Konnerth A, Lux HD, Morad M (1987) Proton-induced transformation of calcium channel in chick dorsal root ganglion cells. J Physiol (Lond) 386:603–633.

Kruh J (1982) Effects of sodium butyrate, a new pharmacological agent, on cells in culture. Mol Cell Biochem 42:65–82.

Kullberg R, Owens JL, Camacho P, Mandel G, Brehm P (1990) Multiple conductance classes of mouse nicotinic acetylcholine receptors expressed in *Xenopus* oocytes. Proc Natl Acad Sci USA 87:2067–2071.

Loring RH, Salpeter MM (1980) Denervation increases turnover rate of junctional acetylcholine receptors. Proc Natl Acad Sci USA 77: 2293–2297.

Miles K, Anthony DT, Rubin LL, Greengard P, Huganir RL (1987) Regulation of nicotinic acetylcholine receptor phosphorylation in rat myotubes by forskolin and cAMP. Proc Natl Acad Sci USA 84:6591–6595.

Mishina M, Takai T, Imoto K, Noda M, Takahashi T, Numa S, Methfessel C, Sakmann B (1986) Molecular distinction between fetal and adult forms of muscle acetylcholine receptor. Nature 321:406–410.

Miyawaki A, Furuichi T, Maeda N, Mikoshiba K (1990) Expressed cerebellar-type inositol 1,4,5-trisphosphate receptor, P_{400}, has calcium release activity in a fibroblast L cell line. Neuron 5:11–18.

Nomoto H, Takahashi N, Nagaki Y, Endo S, Arata Y, Hayashi K (1986) Carbohydrate structures of acetylcholine receptor from *Torpedo californica* and distribution of oligosaccharides among the subunits. Eur J Biochem 257:233–242.

Patrick J, McMillan J, Wolfson H, O'Brien JC (1977) Acetylcholine receptor metabolism in a nonfusing muscle cell line. J Biol Chem 252:2143–2153.

Phillips WD, Kopta C, Blount P, Gardner PD, Steinbach JH, Merlie JP (1991) Acetylcholine receptor-rich membrane domains organized in fibroblasts by recombinant 43-kD protein. Science 251:568–570.

Reiness CG, Weinberg CB (1981) Metabolic stabilization of acetylcholine receptors at newly formed neuromuscular junctions in rat. Dev Biol 84:247–254.

Schuetze SM, Role LW (1987) Developmental regulation of nicotinic acetylcholine receptor. Annu Rev Neurosci 10:403–457.

Shyng S-L, Xu R, Salpeter MM (1991) Cyclic AMP stabilizes the degradation of original junctional acetylcholine receptors in denervated muscle. Neuron 6:469–475.

Sine SM, Claudio T (1991a) Stable expression of the mouse nicotinic acetylcholine receptor in mouse fibroblasts. J Biol Chem 266:13679–13689.

Sine SM, Claudio T (1991b) γ- and δ-subunits regulate the affinity and the cooperativity of ligand binding to the acetylcholine receptor. J Biol Chem 266:19369–19377.

Sine SM, Taylor P (1979) Functional consequences of agonist-mediated state transitions in the cholinergic receptor. J Biol Chem 254: 3315–3325.

Sine SM, Taylor P (1981) Relationship between reversible antagonist occupancy and the functional capacity of the acetylcholine receptor. J Biol Chem 256:6692–6699.

Smith MM, Schlesinger S, Lindstrom J, Merlie JP (1986) The effects of inhibiting oligosaccharide trimming by 1-deoxynojirimycin on the nicotinic acetylcholine receptor. J Biol Chem 261:14825–14832.

Smith MM, Merlie JP, Lawrence JC Jr (1987) Regulation of phosphorylation of nicotinic acetylcholine receptors in mouse BC3H-1 myocytes. Proc Natl Acad Sci USA 84:6601–6605.

Smith MM, Merlie JP, Lawrence JC Jr (1989) Ca^{2+}-dependent and cAMP-dependent control of nicotinic acetylcholine receptor phosphorylation in muscle cells. J Biol Chem 264:12813–12819.

Steinbach JH (1981) Neuromuscular junctions and α-bungarotoxin-binding sites in denervated and contralateral cat skeletal muscles. J Physiol (Lond) 313:513–528.

Steinbach JH (1989) Structural and functional diversity in vertebrate skeletal muscle nicotinic acetylcholine receptors. Annu Rev Physiol 51:353–365.

Steinbach JH, Bloch RJ (1986) The distribution of acetylcholine receptors on vertebrate skeletal muscle cells. In: Receptors in cellular recognition and developmental processes. (Gorczynski RM, ed), pp 183–213. New York: Academic.

Tzartos SJ, Rand DE, Einarson BL, Lindstrom JM (1981) Mapping

of surface structures of *Electrophorus* acetylcholine receptor using monoclonal antibodies. J Biol Chem 256:8635–8645.
Vandlen RL, Wu WC-S, Eisenach JC, Raftery MA (1979) Studies of the composition of purified *Torpedo californica* acetylcholine receptor and of its subunits. Biochemistry 18:1845–1854.
Welinder C, Larsson N-G, Szigeti R, Ehlin-Henriksson B, Henle G, Henle W, Klein G, Ricksten A, Rymo L, Sulitzeanu D (1987) Stable transfection of a human lymphoma line by sub-genomic fragments of Epstein-Barr virus DNA to measure humoral and cellular immunity to the corresponding proteins. Int J Cancer 40:389–395.
Ziskind L, Dennis MJ (1978) Depolarising effect of curare on embryonic rat muscles. Nature 276:622–623.